Supporting information

Reversing activity of cancer associated fibroblast for staged glycolipid micelles

against internal breast tumor cells

Yun Zhu,[†] Fangying Yu,[‡] Yanan Tan,[†] Yun Hong,[§] Tingting Meng,[‡] Yupeng Liu,[‡] Suhuan Dai,[‡] Guoxi Qiu,[‡] Hong Yuan,[‡] and Fuqiang Hu*[†‡]

[‡]College of Pharmaceutical Science, Zhejiang University, 866 Yuhangtang Road, Hangzhou 310058, People's Republic of China.

[†] Ocean College, Zhejiang University, 1 Zheda Road, Zhoushan 316021, People's Republic of China.

[§] The First Affiliated Hospital, College of Medicine, Zhejiang University, 79 Qingchun Road, Hangzhou 310058, China

*Corresponding Author: Prof. Fuqiang Hu

Tel/Fax: +86-571-88208439

E-mail: hufq@zju.edu.cn
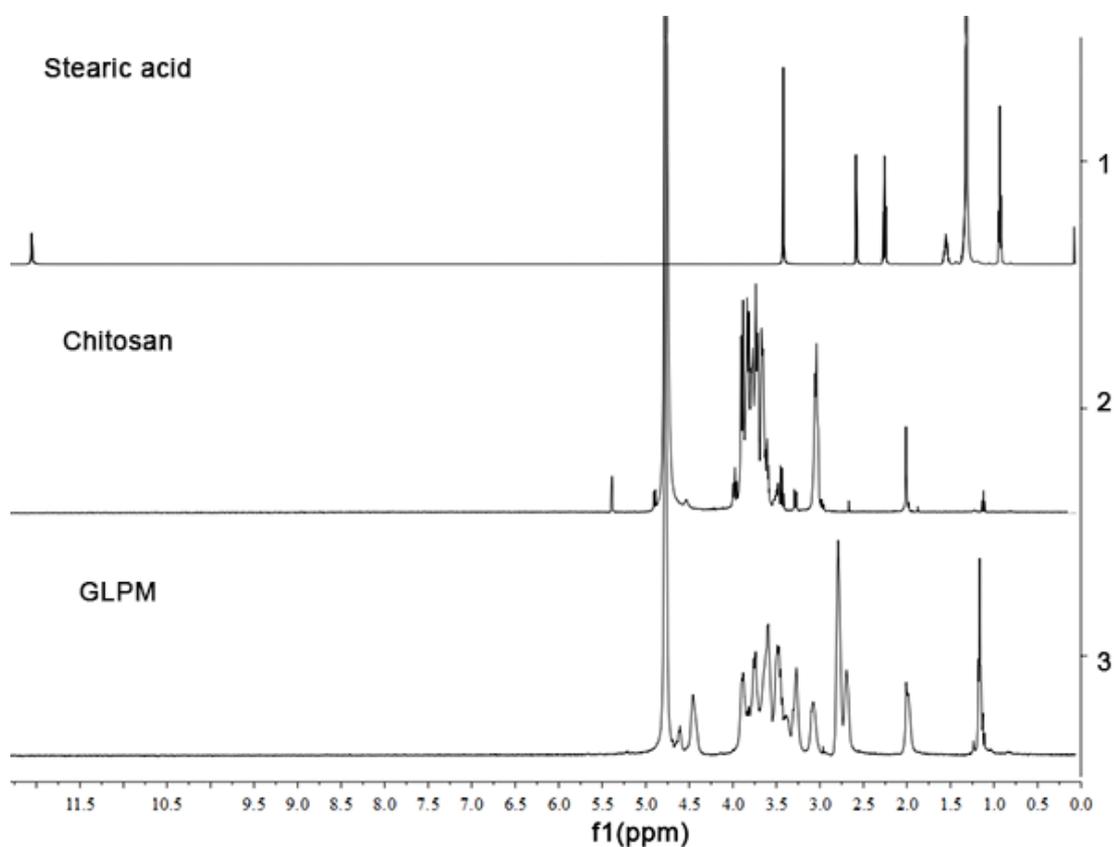
Figure S1. The 1H NMR spectroscopy of synthesized glycolipid polymer.
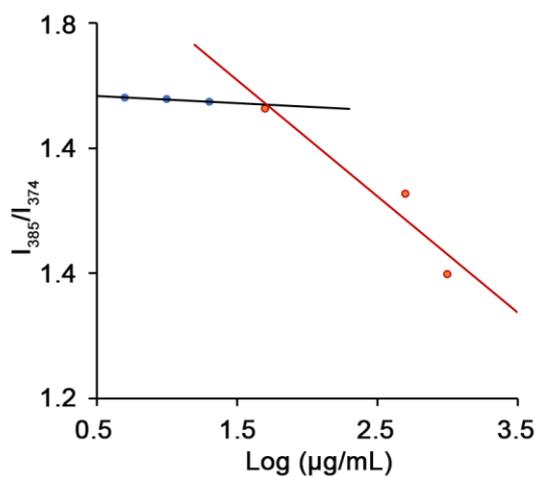
Figure S2. CMC value of GLPM in aqueous medium.
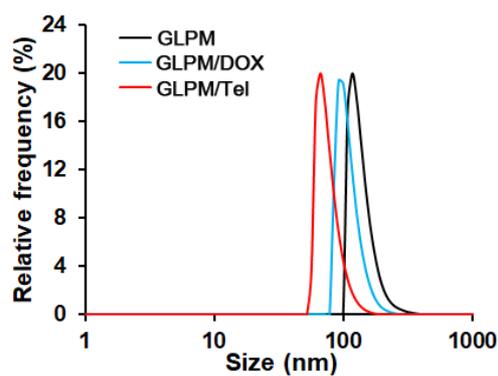
Figure S3. The size of GLPM, GLPM/DOX and GLPM/Tel measured by DLS.
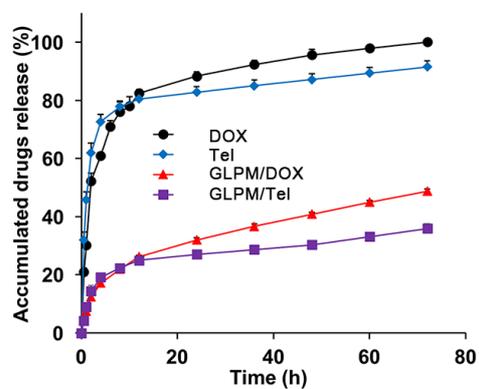
Figure S4. Drug release profiles of Tel, DOX, GLPM/Tel and GLPM/DOX after incubation with pH 7.4 PBS (10% fetal bovine serum).
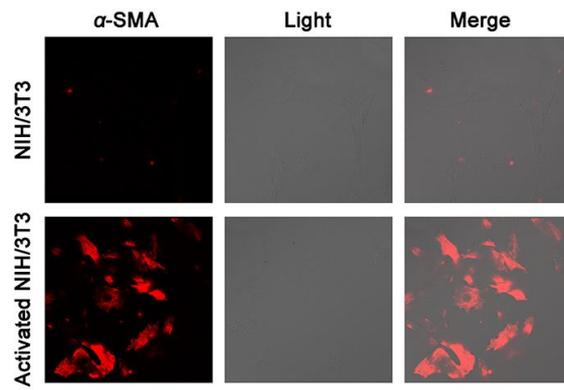
Figure S5. The activation of normal NIH/3T3 cells by supernatant collected from MCF-7 cells.
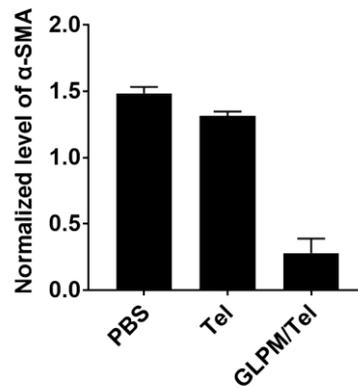
Figure S6. Semi-quantitative analysis of expressed α-SMA in activated NIH/3T3 cells after different drugs treatment.
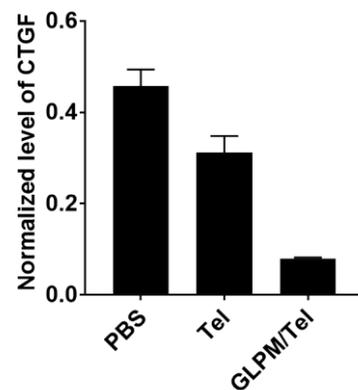
Figure S7. Semi-quantitative analysis of expressed CTGF in activated NIH/3T3 cells after different drugs treatment.
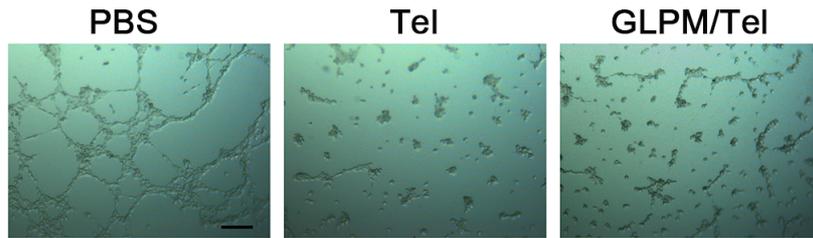
Figure S8. The anti-angiogenic efficacy of Tel and GLPM/Tel on HUVEC cell line *in vitro*.
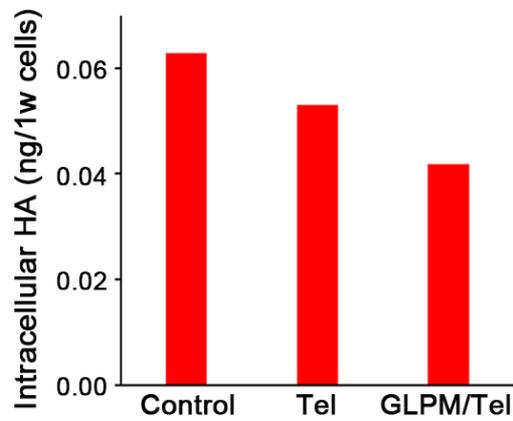
Figure S9. Quantitative analysis of intracellular HA after drugs treatment for 48h.
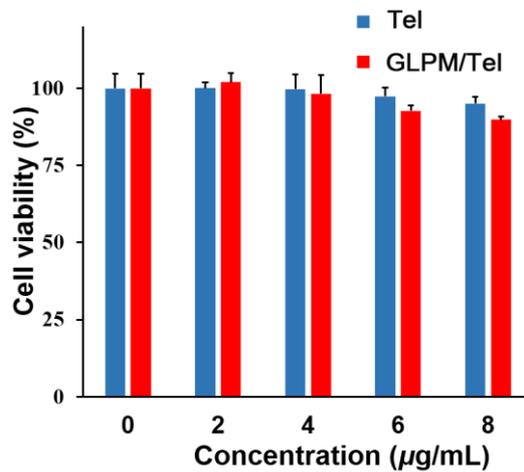
Figure S10. Cytotoxicity evaluation of Tel and GLPM/Tel on activated NIH/3T3 cell.
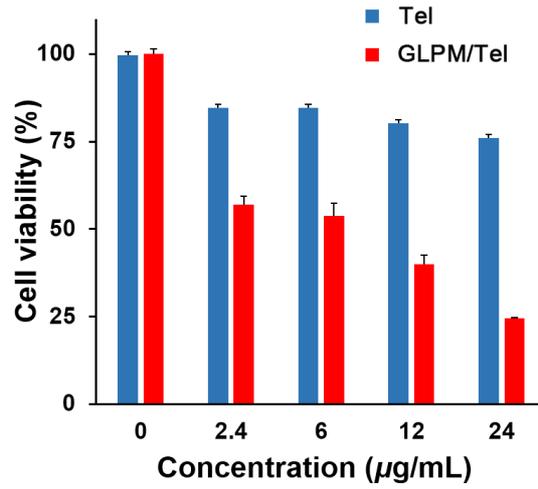
Figure S11. Cytotoxicity evaluation of Tel and GLPM/Tel on MCF-7 cell.
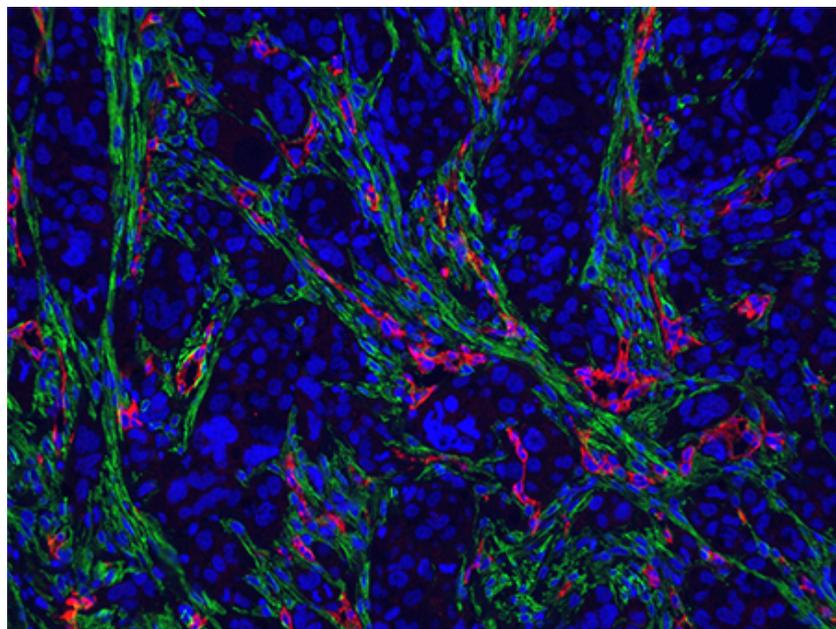
Blue: cell nucleus   Green: α-SMA   Red: CD31

Figure S12. Immunofluorescent staining for the pathological structure on MCF-7 tumor mass.
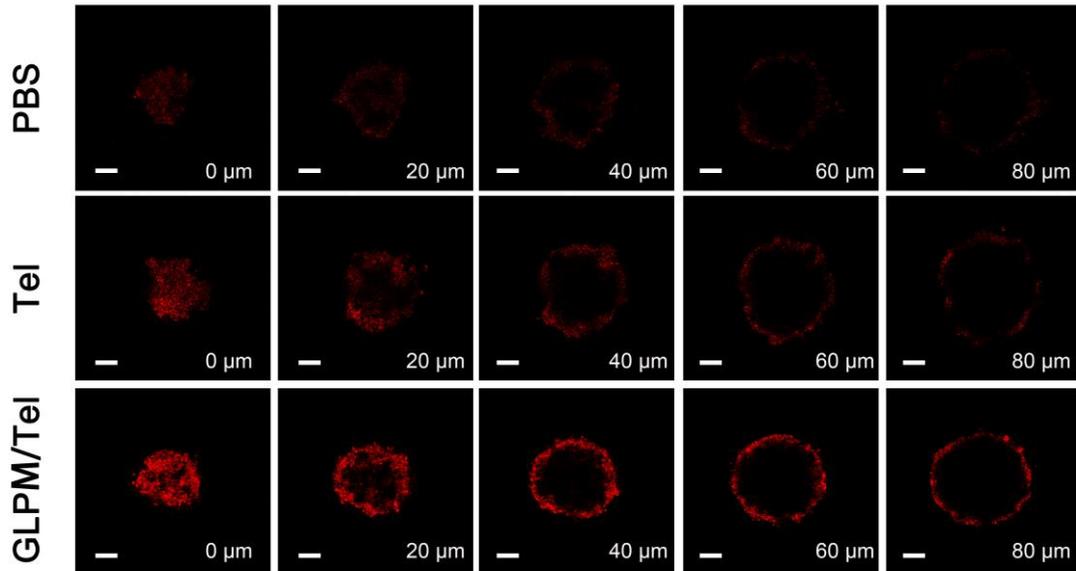
Figure S13. Z-stack images of penetration of GLPM/DOX in MCTSs composed of 4T1 cells and activated NIH/3T3 cells were visualized by confocal microscopy after PBS, Tel and GLPM/Tel treatment for 2 days. Bars: 100 μm.
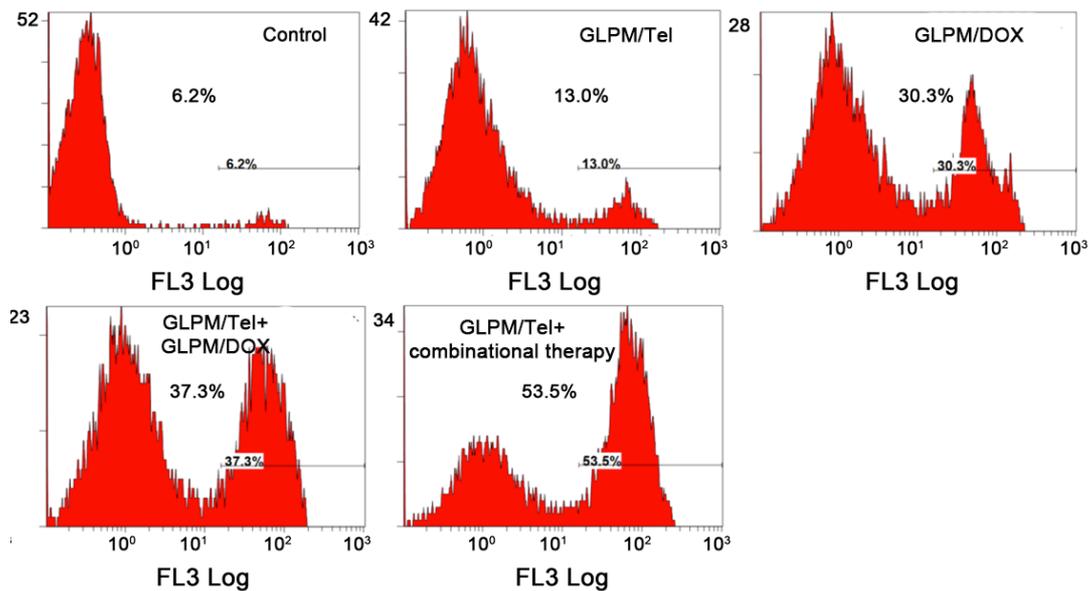
Figure S14. Antitumor efficacy of different drugs on MCTSs measured by PI staining.
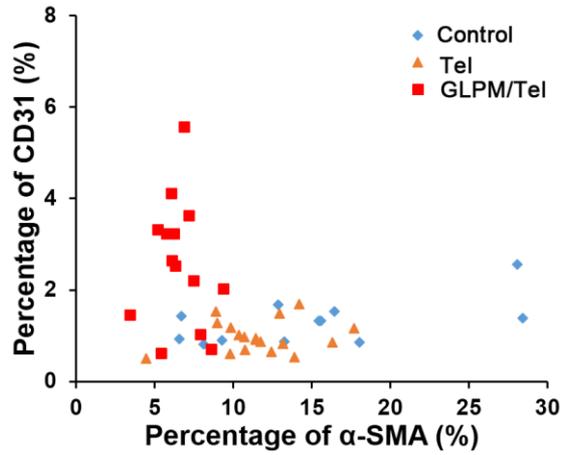
Figure S15. The correlation between α-SMA and CD31 calculated by imageJ software.
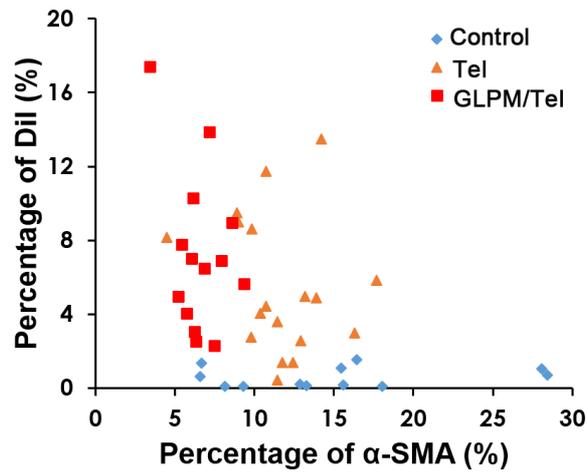
Figure S16. The correlation between α-SMA and DiI calculated by imageJ software.
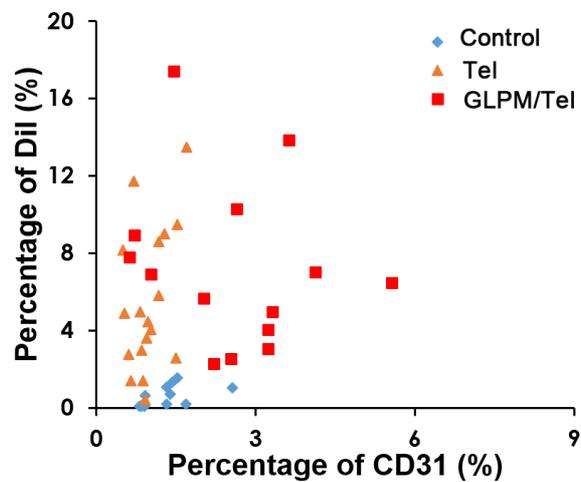
Figure S17. The correlation between CD31 and DiI calculated by imageJ software.
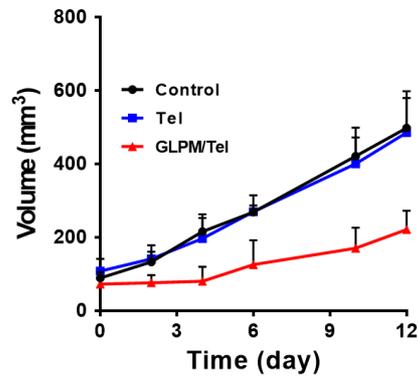
Figure S18. The volumes of MCF-7 tumor during saline, Tel and GLPM/Tel treatments.
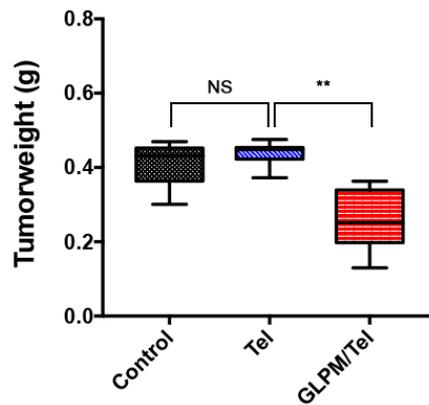
Figure S19. The weight of MCF-7 tumor masses after saline, Tel and GLPM/Tel treatment for three times. **p < 0.01, ***p < 0.001 as determined by two-tailed student's t-test.
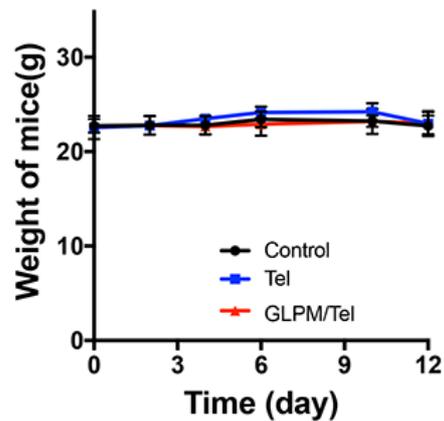
Figure S20. The weight of mice during drugs treatment.
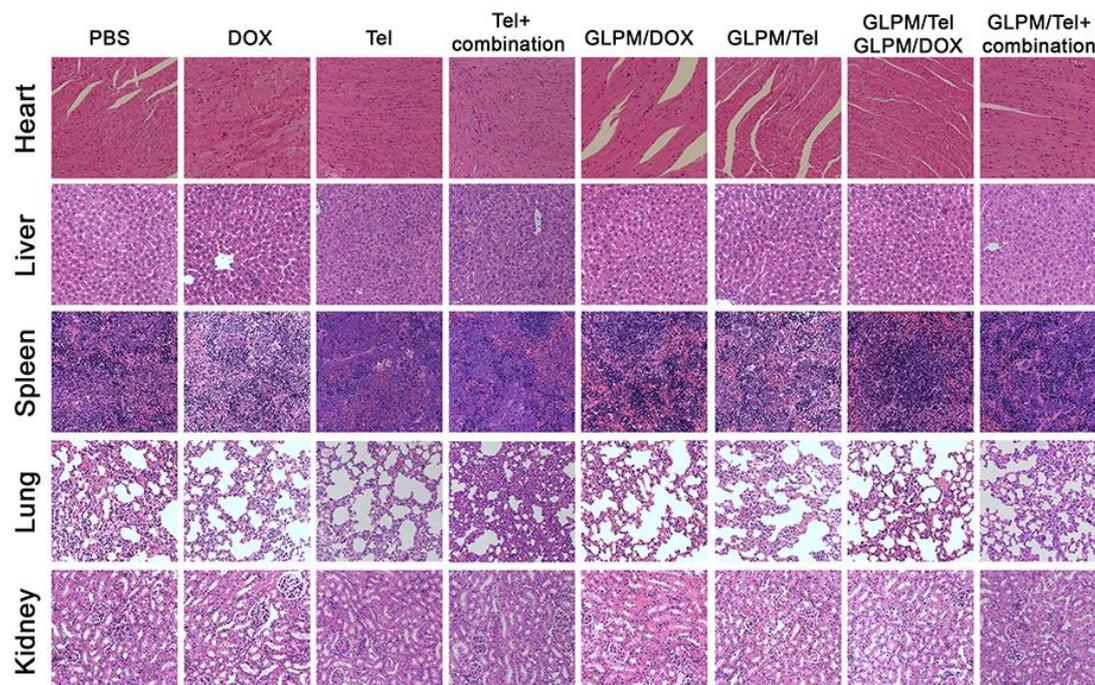
Figure S21. HE staining for major organs after drugs treatment.

Table S1. Depth of MCTSs after drugs treatment.

	PBS	Tel	GLPM/Tel	GLPM/DOX	GLPM/Tel+ GLPM/DOX	GLPM/Tel+ combinational therapy
Penetration Depth	70μm	140μm	140μm	/	/	/
Apoptosis ratio	6.2%	/	13.0%	30.3%	37.3%	53.5%